JOURNAL OF Materials CHEMISTRY

Hydrothermal synthesis and characterisation of $BaTiO_3$ fine powders: precursors, polymorphism and properties†

Iain J. Clark,[a] Tomanari Takeuchi,[b] Noikazu Ohtori[c] and Derek C. Sinclair[a]

[a]*Chemistry Department, University of Aberdeen, Meston Walk, Aberdeen, UK AB24 3UE*
[b]*Osaka National Research Institute, 1–8-31, Midorigaoka, Ikeda, Osaka, Japan*
[c]*Graduate School of Science and Technology, Niigatu University, Ikarashi 2-no cho, Niigata, Japan*

Received 19th June 1998, Accepted 22nd July 1998

The influence of two Ti-precursors, TiO_2 (anatase) and H_2TiO_3 (β-titanic acid), on the purity and particle size of $BaTiO_3$ powders prepared *via* hydrothermal synthesis is discussed. Amorphous H_2TiO_3 was found to be an excellent Ti-precursor material and offers several advantages over crystalline anatase. Phase pure powders which have small particle sizes, *ca.* 40–80 nm and narrow particle size distributions can be prepared at 180 °C after 24 h using H_2TiO_3 as a precursor material. Although the initial reaction is very fast, *ca.* 90% yield after 8–10 h, extended reaction periods at 180 °C are required in order to drive the reaction to completion. Lowering the reaction temperature from 180 to 85 °C does produce powders with even smaller particle sizes, however, very long reaction periods are required, *e.g.* >72 h, to ensure complete reaction. Raman spectra of as-prepared and heat treated (1000 °C) powders with average particle sizes as small as *ca.* 20–40 nm indicate asymmetry within the TiO_6 octahedra of the $BaTiO_3$ lattice. These results contradict the widely cited 'critical' particle size theory for the stabilisation of the cubic polymorph, at least for particle sizes greater than *ca.* 20–40 nm. As-prepared powders contain many defects, primarily in the form of lattice OH^- ions. Preliminary ac impedance spectroscopy data on samples heat treated to remove lattice hydoxyl ions demonstrate these materials to be modest proton conductors.

Introduction

$BaTiO_3$ is one of the most widely used and studied ferroelectric materials in the electro-ceramics industry. It has various polymorphs, all of which are based on the perovskite structure;[1] however, the two most studied are the tetragonal, t, and cubic, c, polymorphs. t-$BaTiO_3$ forms between *ca.* 0 and 130 °C whereas c-$BaTiO_3$ is stable above 130 °C. In the t-polymorph, titanium ions are displaced from the centrosymmetric position within TiO_6 octahedra and give rise to spontaneous polarisation. Due to this asymmetry within the crystal structure, t-$BaTiO_3$-based materials have high permittivities and are widely employed as dielectrics in ceramic capacitors.[2] The transition from the polar (ferroelectric) t- to non-polar (paraelectric) c-polymorph normally occurs at *ca.* 130 °C, the Curie temperature, T_c. Above T_c, the Ti ions occupy, on average, the centrosymmetric position within TiO_6 octahedra and there is no net polarisation within the solid.

A typical room temperature permittivity value, ε_{25}, for ceramic t-$BaTiO_3$ with an average grain size of *ca.* 10 μm is 1000–2000; however, this rises sharply to a maximum value, ε_{max}, of *ca.* 10 000 at T_c. In such 'large' grained ceramics, a variety of ferroelectric domain structures form to relieve internal stress associated with the cubic to tetragonal phase transformation. Although a detailed discussion of domain structures in $BaTiO_3$ powders and ceramics is outwith the scope of this paper, it is important to note that ferroelectric domain structures and dipole–dipole interactions control the permittivity characteristics of $BaTiO_3$ and that these depend on particle or grain size. For example, Arlt *et al.*[3] have shown that ε_{25} for $BaTiO_3$ ceramics can be optimised to a value approaching 5000 by controlling the grain size to be *ca.* 0.7–1.0 μm.

Several models have been proposed to explain this grain size effect but there is still no clear consensus as to its origin.‡ Two commonly cited models involve the generation of higher-than-usual stress in fine grained ceramics[5,6] whereas a third suggests a core-shell structure,[7,8] whereby grains below a 'critical' size (<0.2 μm) have cubic symmetry, intermediate grain sizes (*ca.* 1 μm) have a ferroelectric-tetragonal core with a cubic surface layer and large grains (5 μm) are essentially tetragonal. It should be noted that there is not an accepted 'critical' particle or grain size below which the cubic polymorph is stabilised, on the contrary, a wide range of values, *ca.* 25–190 nm have been reported.[9–16] In addition, a variety of reasons have been proposed for the room-temperature stabilisation of the cubic polymorph, including the presence of lattice 'defects' such as hydroxyl ions[17] (associated with powders formed *via* wet chemical methods), small deviations in Ba/Ti stoichiometry[7] and excess surface energy associated with ultrafine particles.[18,19] Clearly, much remains to be done in order to establish the factors which influence and control the crystal symmetry and electrical properties of sub-micron $BaTiO_3$ powders and ceramics.

Despite these fundamental problems, $BaTiO_3$ will continue to be used in the manufacture of thermistors,[20] multilayer capacitors,[21] electro-optic devices[22] and DRAM (dynamic random access memories)[23] into the next century. Improved performance and miniaturisation of $BaTiO_3$-based devices, either in the form of thin ceramic layers, *ca.* 20 μm, for multilayer capacitors or as thin films for integrated electronic circuits remains a priority. High permittivities and miniaturisation can be achieved by controlling the ceramic microstructure which, in turn, depends on the homogeneity, composition, surface area and particle size of the starting $BaTiO_3$ powder. In addition, it is well known that $BaTiO_3$ undergoes exaggerated grain growth during sintering at elevated temperatures and long sintering periods. This can produce ceramics

†Basis of the presentation given at Materials Chemistry Discussion No. 1, 24–26 September 1998, ICMCB, University of Bordeaux, France.

‡During the preparation of this manuscript, Frey *et al.*[4] published a paper which appears to have clarified many of the problems associated with the origin of the so-called grain size effect in $BaTiO_3$.

containing very large grain sizes, *e.g.* >50 μm or duplex microstructures of low density consisting of both large (>10 μm) and small (<1 μm) grains. For these reasons, many synthetic methods and sintering profiles[24–28] have been investigated in an attempt to produce sub-micron, deagglomerated fine powders of $BaTiO_3$ that can be sintered into dense, fine-grained ceramics.

Traditionally, $BaTiO_3$ has been produced *via* the mixed oxide route. This method involves repeated calcination and regrinding of $BaCO_3$ and TiO_2 powders above 1100 °C. The reaction mechanism in air has been proposed to take place in at least three stages[29–32] and relies on the diffusion of Ba^{2+} ions into TiO_2. Firstly, $BaCO_3$ reacts with the outer surface regions of TiO_2 to form a surface layer of $BaTiO_3$ on individual TiO_2 grains. Further diffusion of Ba^{2+} ions into TiO_2 necessitates the formation of Ba_2TiO_4 between unreacted $BaCO_3$ and the previously formed $BaTiO_3$. After prolonged sintering periods, the intermediate Ba-rich phase Ba_2TiO_4 reacts with the remaining TiO_2 in the core-regions of the TiO_2 grains to form $BaTiO_3$. Although the nominal starting Ba/Ti ratio is 1:1, long reaction times are required to form homogeneous powders free from secondary phases. For such a complex and slow reaction mechanism, it is desirable to have high surface area TiO_2 powders of fine particle size and narrow size distribution in order to control the morphology and grain size of the resultant $BaTiO_3$ powder. Nevertheless, the mixed oxide route tends to produce coarse, agglomerated powders that require high sintering temperatures to form dense ceramics.

In order to produce powders that are suitable for sintering into micron-grain-sized ceramics for MLC applications there has been much interest in developing wet and novel chemical routes. As these reactions take place in the liquid, as opposed to the solid state, more intimate mixing of the cations is achieved and consequently, much shorter diffusion pathways are created. Deagglomerated, sub-micron powders of $BaTiO_3$ can then be obtained at low temperatures and short reaction periods, for example *via* hydrothermal synthesis at 240 °C for 24 h.[33] Other common methods include, oxalate (Clabauch),[34] citrate (Pechini),[35] catecholate (Milne)[36] and sol–gel.[37] Although the reaction mechanisms and advantages and disadvantages of many of these routes have been discussed,[38] for the present purposes it is worth discussing these issues for hydrothermal synthesis.

$BaTiO_3$ powders have been prepared *via* hydrothermal processing since the 1940's and this method is commonly employed to produce commercial powders. Although it is well established that $BaTiO_3$ is the only thermodynamically stable binary compound produced under all conditions,[39] *i.e.* pH, Ba/Ti ratio, reaction temperature, *etc.* products can contain unreacted TiO_2 and $BaCO_3$. Normally, an excess of Ba^{2+} in the starting solution is employed (Ba/Ti = 1.05–1.10:1) in an attempt to remove any unreacted TiO_2 and therefore drive the reaction to completion. Any excess Ba, in the form of $BaCO_3$ can then be removed *via* acid washing of the powders. Although this procedure is effective in controlling the purity of the powders, relatively little is known about the influence of acid washing on powder stoichiometry as Ba^{2+} may be leached from the surfaces of the particles. Although controlling the precise stoichiometry of hydrothermal $BaTiO_3$ powders can be problematic, the low cost and easy handling of the reagents, and the fast reaction rate at low temperatures ensures that deagglomerated powders consisting of small particles of narrow size distribution are readily obtained.

Several mechanisms have been proposed for the hydrothermal synthesis of $BaTiO_3$. Hertl[40] has suggested an *in situ* transformation whereby dissolved Ba^{2+} ions react with undissolved TiO_2 to produce a continuous layer of $BaTiO_3$ on the surface of TiO_2 particles. The reaction is then controlled either by diffusion of Ba^{2+} through the product $BaTiO_3$ layer or further reaction between unreacted TiO_2 within grain interiors and the surrounding $BaTiO_3$. For this model, complete reaction may be difficult to achieve due to increasing encapsulation of TiO_2 *via* product formation.

Homogeneous and heterogeneous dissolution–precipitation models have also been proposed. In the homogeneous model, a low concentration of TiO_2 dissolves in the form of soluble hydroxytitanium complexes which then react with Ba^{2+} ions in solution to precipitate $BaTiO_3$. In the heterogeneous model, $BaTiO_3$ nuclei form on the surfaces of the dissolving TiO_2 particles and, as for the *in situ* transformation mechanism, the reaction becomes limited by the increasing isolation of the reactants *via* $BaTiO_3$ product layers on the surface of TiO_2 particles.

Eckert *et al.* reviewed these models[41] in more detail and undertook a kinetic study of hydrothermal reactions involving barium hydroxide octahydrate and anatase precursors. Two reaction regimes were clearly identified; during the early stages the reaction is controlled by a dissolution–precipitation process, whereas, for the second regime at longer reaction times the results were inconclusive. The authors suggest two plausible but different explanations for their kinetic data, one model is based on heterogeneous dissolution–precipitation followed by *in situ* transformation, whereas, the second model suggests that dissolution–precipitation is the controlling mechanism, with nucleation and growth of $BaTiO_3$ controlling the first regime and the dissolution rate of TiO_2 controlling the second regime.

In the present paper we discuss some of our recent work on the hydrothermal synthesis of $BaTiO_3$ powders and highlight some advantages of using amorphous H_2TiO_3 as opposed to crystalline anatase as a precursor material. In particular, H_2TiO_3 promotes faster and more-complete reactions and also produces powders with much smaller particle sizes. We discuss the influence of temperature on the rate of reaction and on the particle size, distribution and water content of the $BaTiO_3$ powders. The importance of using Raman spectroscopy to detect the presence of trace amounts of unreacted Ti-containing precursors and to yield information on the polymorphism of sub-micron powders is discussed. Finally, we present preliminary results on powders and ceramics heat treated above 800 °C that support the idea that hydrothermal $BaTiO_3$ powders contain many defects which influence their physical properties.

Experimental

$Ba(OH)_2 \cdot 8H_2O$ (98+%, Aldrich) and anatase (99.9%, Aldrich) or β-H_2TiO_3 (+99%, Mitsuwa Chemicals) were mixed with a Ba:Ti ratio of 1.05:1 in a 23 ml Teflon-lined pressure vessel (Model 4749, Parr Instruments) together with 10 ml of de-ionised water. The vessel was sealed, shaken and placed in an oven at either 85, 120 or 180 °C for periods ranging from 1 to 72 h. After cooling, the contents of the bomb were diluted in 30 ml of 0.1 M formic acid in an attempt to dissolve any $BaCO_3$ formed by the addition of excess Ba^{2+} to the starting solution. The mixture was vacuum filtered using a Buchner funnel, the residue thoroughly washed with distilled water and dried overnight in air at 120 °C. The percentage yield of $BaTiO_3$ was estimated from the weight of the dried powders.

Phase purity and polymorphism of the $BaTiO_3$ powders were studied by X-ray diffraction (XRD) and Raman spectroscopy. XRD was carried out on a Stoe STADI P automated powder diffractometer employing monochromatic Cu-$K\alpha_1$ radiation and a linear position sensitive detector over the 2θ range 20 to 80°. Cubic and tetragonal polymorphs were distinguished by the splitting of the (200) peak at $2\theta \approx 45°$. Unit cell parameters were obtained by refinement of XRD data. Raman spectroscopy was carried out on a Jobin Yvon T64000 using a 100 mW Ar laser with a wavelength of 514.5 nm. A 300 μm slit and integration time of 5 s were used

giving a resolution of 8.4 cm^{-1}. Spectra were measured over the range 58–1103 cm^{-1}. Impurity phases such as $BaCO_3$ and TiO_2 (anatase) were detected from characteristic peaks at 1060 and 150 cm^{-1}, respectively. The presence of a peak in the spectra of $BaTiO_3$ at 305 cm^{-1} indicates asymmetry within TiO_6 octahedra[42] and was used to distinguish between tetragonal and cubic polymorphs.

Thermogravimetric analysis (TGA) was carried out using a Stanton Redcroft TG-DTA simultaneous thermal analyser (model STA 1000/1500) to determine the water content of as-prepared powders. Samples were accurately weighed to five decimal places in a platinum crucible and weight losses recorded from 25–1000 °C against an alumina reference. All experiments were carried out in air at a heating rate of 10 °C min^{-1} with an amplifier setting of 50 μV.

Powder morphology was determined *via* transmission electron microscopy (TEM) using a JEOL electron microscope (model 2000EX TEMSCAN) operating at 200 kV. Particle size and distribution were obtained by measuring the cross diagonals of approximately 130 particles from scanned negatives of TEM images. Energy dispersive X-ray analysis (EDX) was used in an attempt to determine the Ba : Ti ratio of the $BaTiO_3$ particles and also to detect the presence of any unreacted TiO_2.

Electron probe micro-analysis (EPMA) was employed to determine the homogeneity of sintered pellets fabricated from the various powders. Pellets were sintered at *ca.* 1350 °C and a Cameca SX51 electron microprobe employed using an accelerating voltage of 20 kV and a beam current of 40 nA. Ba-Lα and Ti-Kα lines were measured using benitoite, $BaTiSi_3O_9$, as a standard. Prior to analysis, small pieces of pellet were mounted in resin blocks, surface polished and carbon coated.

Electrical measurements were carried out using a Solartron frequency response analyser (model 1250 or 1260) combined with a Solartron dielectric interface (model 1296). A frequency range of 10^{-3}–10^{6} Hz was employed with an applied voltage of 100 mV. Cold pressed pellets of various powders were sintered between 800 and 1350 °C and organopaste and gold foil electrodes applied to the surfaces of the pellets at 800 °C, prior to mounting in a conductivity jig. Measurements were recorded over the temperature range 25–500 °C.

Before discussing the results it is important to appreciate the need for a wide variety of techniques to determine the phase purity and crystal structure of fine-grain $BaTiO_3$ powders. XRD is an excellent technique for obtaining information on the average or long range crystal structure of a material; however, peak broadening is significant for diffraction from sub-micron sized particles and XRD cannot reveal the very subtle unit cell distortions which occur in $BaTiO_3$ for microdomains of dimensions of *ca.* 100 Å. In addition, routine XRD is relatively insensitive to small quantities of impurity phases, especially for secondary phases which are amorphous/poorly-crystalline and/or have weak X-ray scattering power. In our experience, XRD is sensitive to small quantities of $BaCO_3$ in hydrothermally processed $BaTiO_3$ but is much less sensitive in the detection of unreacted Ti-containing precursors, either crystalline anatase or amorphous H_2TiO_3.

Uncertainties over crystal symmetry can largely be resolved using alternative techniques such as Raman spectroscopy to probe short range order or local symmetry. There are reliable Raman spectra in the literature[42] for various $BaTiO_3$ polymorphs; however, it must be stated that the differences in spectra are rather subtle, especially for the orthorhombic, tetragonal and cubic (at temperatures slightly greater than T_c) polymorphs. In contrast to XRD, Raman spectroscopy is sensitive to the presence of both $BaCO_3$ and unreacted Ti-containing precursors. For these reasons we choose to present Raman spectra, as opposed to XRD patterns to illustrate the phase purity and crystal symmetry of as-prepared $BaTiO_3$ powders.

An important aspect of this work is to obtain homogeneous particles of controlled stoichiometry which can be sintered into dense ceramics of uniform microstructure. The Ba : Ti ratio of the particles is an important parameter but is not readily obtained *via* XRD or Raman spectroscopy. We choose, therefore, to study the phase assemblage and Ba : Ti ratio of the grains in sintered ceramics using EPMA and from this, deduce information about the Ba : Ti ratio of the powders. This is an indirect method for obtaining information on the stoichiometry of the powders, but since neither barium nor titanium are particularly volatile at the sintering temperature, we perceive this method to be valid.

Results and discussion

The results are subdivided into three sections. The first section discusses the influence of two Ti-precursors, TiO_2 (anatase) and H_2TiO_3 (β-titanic acid), on the purity and particle size of the $BaTiO_3$ powders. The second section assesses the role of reaction temperature on the rate of reaction, purity, particle size and water content of $BaTiO_3$ powders prepared from $Ba(OH)_2{\cdot}8H_2O$ and H_2TiO_3. The final section discusses preliminary electrical property measurements on powders heat treated above 800 °C.

I Titanium precursors

One of the major problems associated with the hydrothermal synthesis of $BaTiO_3$ is the low solubility of TiO_2 in the highly alkaline environments, *ca.* pH > 12, required for synthesis. Although it is well documented that different Ti-precursors and reaction temperatures influence the rate of reaction there have been few comprehensive studies on the influence of these parameters on the purity and particle size of hydrothermal powders. Kutty *et al.* suggested that amorphous Ti-precursors react fastest,[17] then anatase with rutile giving the slowest reaction. Various workers reported an increase in average particle size and a change (*via* XRD) from cubic to tetragonal symmetry with increasing reaction temperature.[9–16] We decided to reinvestigate some of these findings by comparing the reaction rates, powder purity and particle size of hydrothermal $BaTiO_3$ powders prepared at various temperatures and reaction periods using two Ti-precursors: amorphous H_2TiO_3 (BET using N_2, surface area 193 m^2 g^{-1}) and crystalline anatase (BET, surface area 8.9 m^2 g^{-1}).

In general, for a set reaction temperature and period, the reaction rate was faster and the average $BaTiO_3$ particle size smaller for reactions using the amorphous H_2TiO_3. Raman spectra of powders prepared under the same conditions for the two precursors are shown in Fig. 1. Spectra of anatase and the tetragonal polymorph of $BaTiO_3$ prepared *via* the traditional mixed oxide route are included for comparison. The Raman spectrum of H_2TiO_3 is not shown but is similar to that of anatase and is also dominated by a large peak at *ca.* 150 cm^{-1}. There are two noticeable features in the Raman spectra of the products which are not readily discernible from the XRD patterns (not shown) and which provide important information.

First, the powder products from the H_2TiO_3 reaction appear to be phase pure $BaTiO_3$, whereas unreacted TiO_2, as shown by the presence of the peak at *ca.* 150 cm^{-1}, is clearly present in the products of the anatase reaction. Small amounts of unreacted anatase or amorphous H_2TiO_3 are difficult to detect *via* routine XRD but are readily detected (by the peak at *ca.* 150 cm^{-1}) in the Raman spectra. This result demonstrates the importance of using Raman spectroscopy to monitor the phase purity of $BaTiO_3$ powders prepared *via* hydrothermal synthesis. We should stress that single phase powders can, in fact, be prepared from crystalline anatase at 180 °C, however the

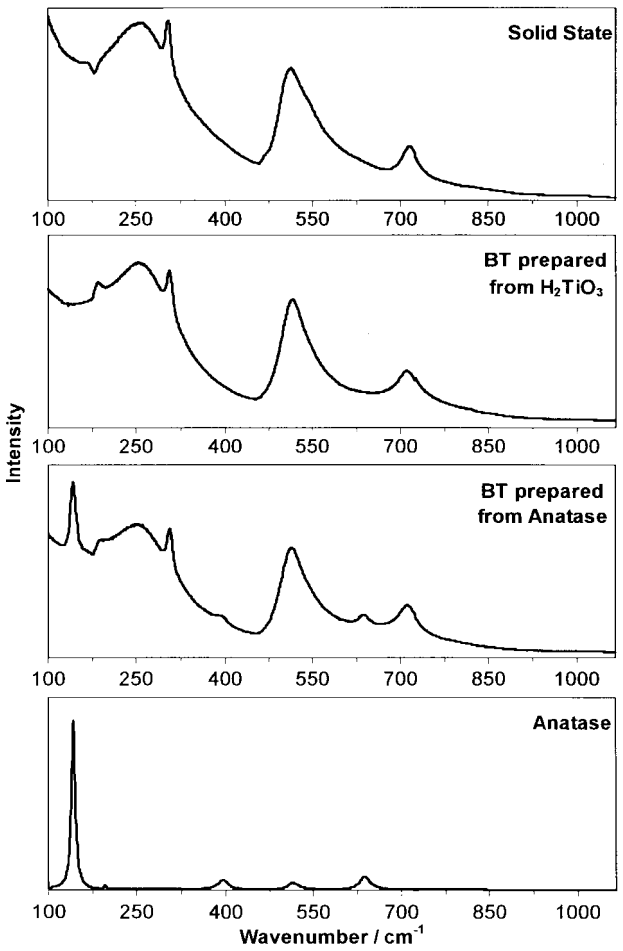

Fig. 1 Raman spectra of $BaTiO_3$ prepared *via* a mixed oxide route (top) and *via* hydrothermal synthesis at 180 °C for 24 h using H_2TiO_3 and anatase as Ti-precursors. The bottom spectrum is of crystalline anatase.

times required are far in excess of those required using amorphous H_2TiO_3, typically in excess of 72 h.

Second, the presence of a peak at 305 cm^{-1} in both spectra indicates asymmetry within the TiO_6 octahedra of $BaTiO_3$ and demonstrates clearly, on a local scale, that as-prepared powders do not have cubic symmetry. In contrast, XRD patterns showed appreciable peak broadening, presumably associated with the small particle size and poor crystallinity of the powders, however, there was little evidence of peak splitting and the XRD data 'appeared' consistent with that for the cubic polymorph, as reported previously.[9–16] The higher sensitivity of Raman spectroscopy to probe the local rather than long range structure clearly demonstrates that sub-micron powders prepared *via* hydrothermal processing are tetragonal rather than cubic.

The particle size of powders prepared from H_2TiO_3 were, on average, 3–5 times smaller than those prepared from TiO_2 and, to our knowledge, are amongst the smallest reported for $BaTiO_3$ powders prepared hydrothermally. Representative micrographs of powders prepared at 180 °C for 24 h from H_2TiO_3 and TiO_2 are shown in Fig. 2 and demonstrate the much smaller particle size, *ca.* 80 nm compared with *ca.* 250 nm. The faster rate of reaction and smaller particle size of powders prepared from amorphous H_2TiO_3 demonstrate two clear advantages of using this precursor instead of crystalline anatase. The remaining sections of the paper concentrate on powders and ceramics prepared using H_2TiO_3 as the Ti-precursor.

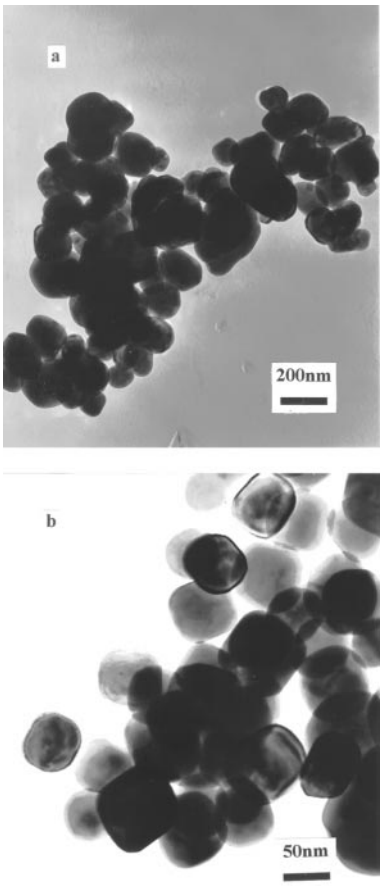

Fig. 2 TEM micrographs of $BaTiO_3$ powders prepared *via* hydrothermal synthesis at 180 °C for 24 h using anatase (a) and H_2TiO_3 (b), as Ti-precursors.

II Reaction temperature

Raman spectra of powder products from two reaction temperatures, 85 and 180 °C after various reaction periods are shown in Fig. 3(a) and (b), respectively. With increasing time, both sets of spectra illustrate a decrease in peak intensity at 150 cm^{-1} associated with the titanium precursor as $BaTiO_3$ is formed. In fact, the spectrum after reaction at 180 °C for 24 h shows no evidence of this peak, suggesting that the reaction has gone to completion. A small peak at 150 cm^{-1} is still apparent in the corresponding spectrum for powders prepared at 85 °C. A higher reaction temperature of *ca.* 180 °C, is clearly required to ensure a more complete reaction for short reaction periods, *e.g.* 24 h. The high surface area (193 m^2 g^{-1}) and the fact that hydroxylation of many Ti–O–Ti bridging bonds has already been achieved in H_2TiO_3, ensure rapid formation of $BaTiO_3$, even at 85 °C. It should be noted that many spectra contained a small peak at 1060 cm^{-1} (not shown) associated with a small amount of $BaCO_3$ which was not completely removed by the mild acid wash.

The weight of the dried powders was used to calculate the percentage yield of $BaTiO_3$ and is shown in Fig. 4. We stress that these values represent upper estimates of the yield, especially for short reaction periods where powders contain unreacted precursor and are also heavily hydrated. Nevertheless, these estimates show that reaction is rapid and yields in excess of 90% are obtained within 8 h of reaction. From the Raman spectra in Fig. 3, extended periods, *e.g.* 24 h at elevated temperatures (180 °C) are required in order to drive the reaction close to completion, even for a reactive precursor such as H_2TiO_3.

As-prepared powders are hydrated and lose water both adsorbed and structural on heating to *ca.* 1000 °C. In general,

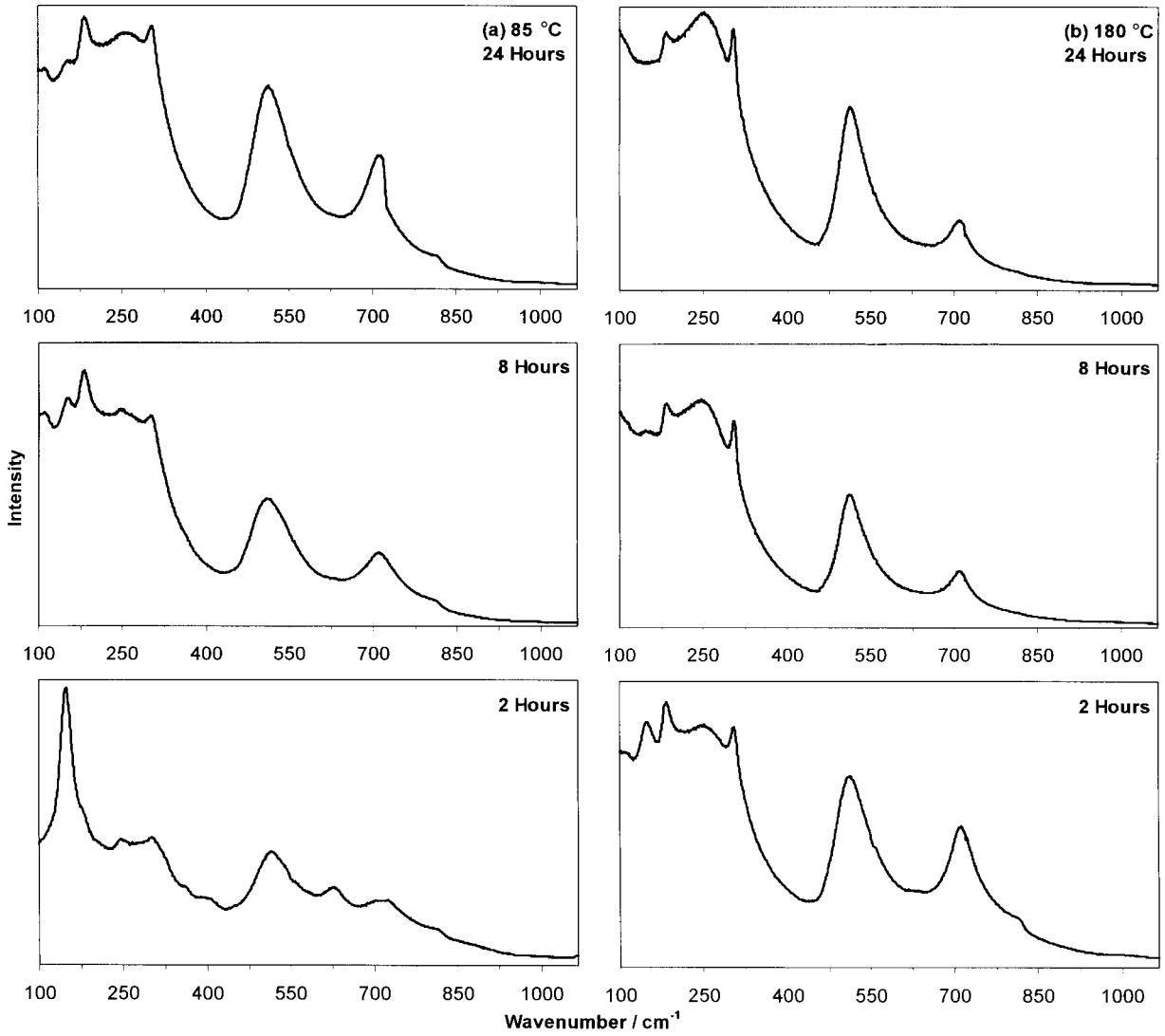

Fig. 3 Raman spectra of powder products from two reaction temperatures, 85 (a) and 180 °C (b), after various reaction periods.

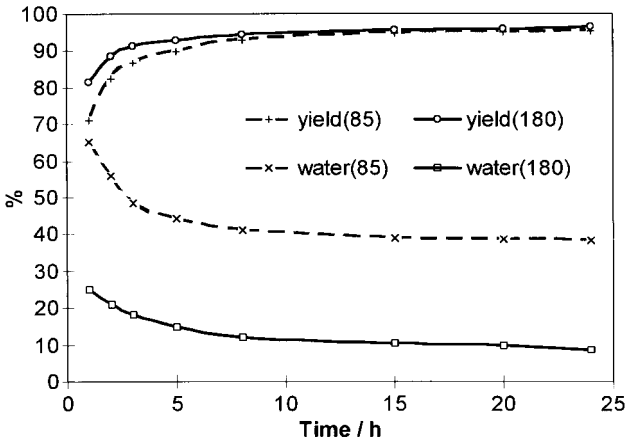

Fig. 4 Percentage yield (weight%) of powder products from reactions at 85 and 180 °C and their associated water content (mol%) as a function of reaction period.

weight loss commenced at *ca.* 100 °C and was complete at *ca.* 600 °C. The powders prepared at 85 °C clearly contained substantially more water, especially for short reaction periods where up to 4 weight% loss was recorded. The water content of powders for each reaction temperature remained reasonably constant after *ca.* 8 h, Fig. 4. This coincides with the dramatic decrease in reaction rate after *ca.* 8–10 h, as shown by the percentage yield of $BaTiO_3$. Nucleation of $BaTiO_3$ crystals presumably takes place *via* a structural rearrangement of the amorphous H_2TiO_3 associated with the incorporation of Ba^{2+} or *via* direct reaction in solution of dissolved hydroxytitanium complexes with Ba^{2+} ions. Either way, the reaction involves dehydration, for example, for the rearrangement mechanism (1).

$$H_2TiO_3 + Ba^{2+} + 2OH^- \rightarrow BaTiO_3 + H_2O \quad (1)$$

Dehydration is slow in superheated fluids and leads to partial retention of H_2O and OH^- in $BaTiO_3$, especially for powders prepared at low temperatures.

The variation in particle size as a function of temperature and time are shown in Fig. 5. All powders have narrow particle size distribution ranges and for each temperature, the mean particle size approximately doubles over a period of *ca.* 20 h, *e.g.* 23 ± 5 to 43 ± 12 nm, between 2 and 24 h at 85 °C and from 53 ± 14 to 80 ± 15 nm at 180 °C. Particle size values after reaction at 120 °C were intermediate between those at 85 and 180 °C. On comparing the particle size values with the variations in product yield, it appears that after an initial 'burst' of nucleation, growth of $BaTiO_3$ particles is a rather slow process.

Micrographs of powders obtained at 85 and 180 °C for 2 h are shown in Fig. 6. At 85 °C, they have poor crystallinity and ill-defined morphology, Fig. 6(a), whereas at 180 °C they are

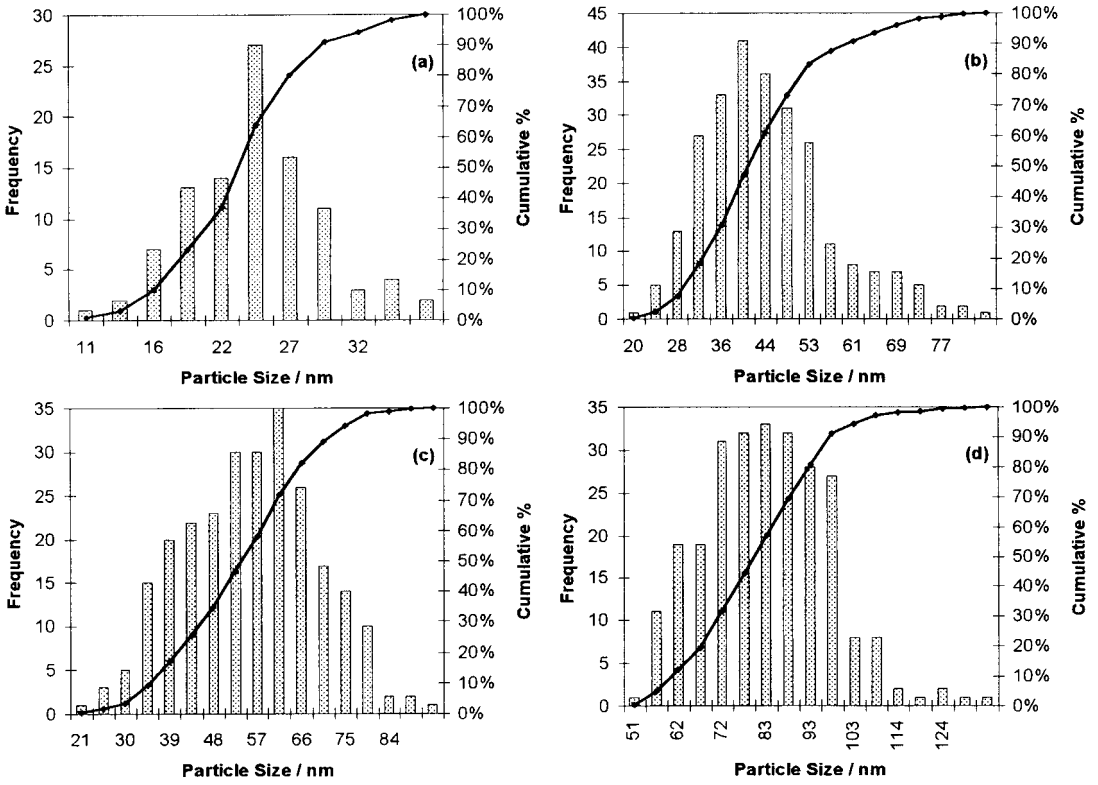

Fig. 5 Particle size histograms for powders prepared at 85 °C after 2 (a) and 24 h (b) and at 180 °C after 2 (c) and 24 h (d).

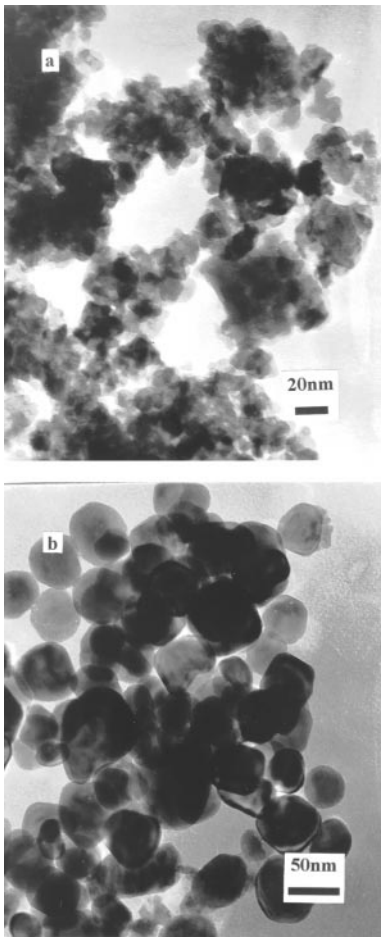

Fig. 6 TEM micrographs of powders prepared at 85 (a) and 180 °C (b), after a reaction period of 2 h.

well-defined, regular particles, Fig. 6(b). The powders prepared at 85 °C have a higher water content and presumably, a higher concentration of lattice defects, such as OH^- ions. Despite the poor crystallinity of such powders, the presence of the peak at 305 cm^{-1} in all Raman spectra, Fig. 3(a), demonstrates that these small particles, *ca.* 20 nm, are tetragonal rather than cubic. This result suggests that the widely-cited 'critical' particle/grain size model is incorrect and that distortion of Ti–O bonds within the $BaTiO_3$ lattice is possible, even for particles as small as *ca.* 20 nm and which contain substantial amounts of lattice defects, such as OH^- ions.

Although our results clarify some of the existing problems in the literature we are unable, at this stage, to identify the reaction mechanism(s) involved in hydrothermal synthesis of $BaTiO_3$. In the final section we discuss some of the properties of heat treated, hydrothermal $BaTiO_3$ powders.

III Heat treated powders

Hydroxyl ions play an important role in the synthesis of $BaTiO_3$ *via* hydrothermal processing, as high pH environments, >12, are required to obtain single phase materials. Infrared spectroscopy[17,43,44] and TGA[45] have both been employed to demonstrate that as-prepared hydrothermal powders contain weakly-bound water molecules adsorbed onto particle surfaces and more strongly bonded structural water in the form of lattice OH^- ions. In general, only total water contents are reported as deconvolution into the two distinct types is difficult. In order to maintain electro-neutrality, it is generally accepted that barium vacancies (V_{Ba}'') are created on the surfaces of individual particles[46] to compensate for the incorporation of lattice OH^- ions on O^{2-} sites ($OH_O^{\bullet}$), according to eqn. (2).

$$2[OH_O^{\bullet}] = V_{Ba}'' \quad (2)$$

On heating above *ca.* 300 °C, lattice OH^- ions are removed as follows,

$$2OH_O^{\bullet} \rightarrow O_o^x + V_O^{\bullet\bullet} + H_2O\ (g) \quad (3)$$

resulting in powders which contain significant concentrations of V_{Ba}'' and $V_O^{\bullet\bullet}$. High concentrations of lattice hydroxyl ions in as-prepared hydrothermal powders therefore influence the stoichiometry (Ba/Ti ratio), defect chemistry and grain growth of sintered $BaTiO_3$ ceramics.

Elimination of water in our powders was complete by *ca.* 600 °C, but there were no significant changes in the Raman spectra of the dehydrated powders until samples were heated >1000 °C. These subtle changes in spectra will be discussed elsewhere,[47] however, the peak at 305 cm^{-1} was present in all processed powders, indicating the distorted crystal symmetry of the particles, irrespective of the presence of adsorbed water or lattice hydroxyl ions. This result contradicts the suggestion that lattice hydroxyl ions play a crucial role in controlling the crystal symmetry of hydrothermal $BaTiO_3$ powders[17,44,45] and is in agreement with the work of Frey and Payne who came to the same conclusion for $BaTiO_3$ powders prepared *via* a sol–gel route.[48]

A selection of XRD patterns over a limited 2θ range for powders prepared at 85 °C and heated up to 1100 °C are shown in Fig. 7. At 800 °C, the broad peak at *ca.* 45.2° (in as-made hydrated powders) sharpens but clear splitting is not apparent until heating at *ca.* 1100 °C. In general, XRD reflections become sharper and more intense after heating at higher temperatures. XRD patterns for powders heated above 1100 °C were indexed on a tetragonal unit cell, whereas, all others were indexed on a cubic unit cell. Lattice parameters and *c*/*a* ratios are shown in Fig. 8 and demonstrate that powders heated at temperatures >1100 °C have *c*/*a* ratios of *ca.* 1.01, which is in good agreement with those reported in the literature.[7]

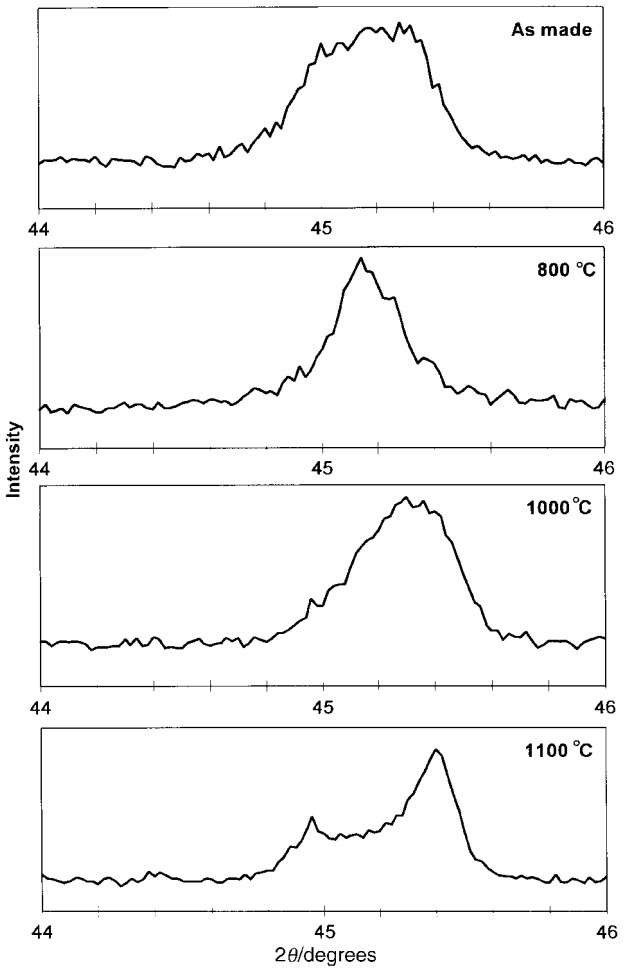

Fig. 7 XRD diffractograms over the 2θ range 44–46° of $BaTiO_3$ prepared at 85 °C (top) and after heat treatment at 800, 1000 and 1100 °C.

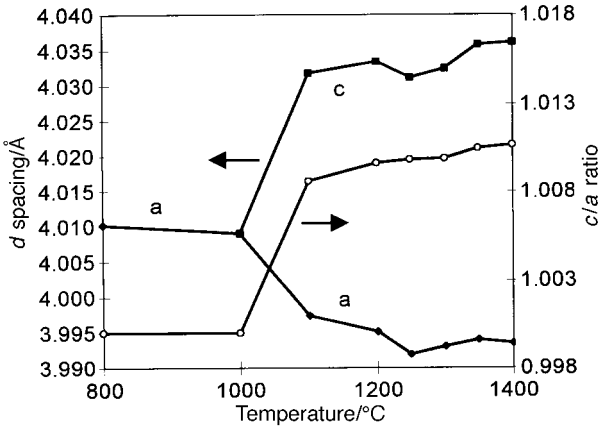

Fig. 8 Lattice parameters (■) and *c*/*a* ratio (○) of $BaTiO_3$ powders prepared at 85 °C for 72 h as a function of processing temperature.

As mentioned previously, cation and anion defects influence the stoichiometry, grain growth and electrical properties of $BaTiO_3$ powders. The diffusion coefficients for oxygen and barium vacancies in $BaTiO_3$ become appreciable above 800 and 1100 °C, respectively. Thus, on heating hydrothermal powders at elevated temperatures, any barium deficiency, either as compensating cation defects for lattice hydroxyl ions or as a consequence of acid washing, or excess titanium, in the form of unreacted Ti-containing precursor, should result in the formation of Ti-rich phases. EPMA and SEM on ceramic pellets sintered at 1350 °C from the powders produced at 85 and 180 °C after 24 h, both demonstrated the existence of Ti-rich secondary phases.

For powders produced at 85 °C, where unreacted TiO_2 was detected *via* Raman spectroscopy, Fig. 3(a), secondary phases were clearly visible as dark intergranular regions in back scattered electron images (BSE), Fig. 9(a). EPMA results identified the presence of both $BaTi_2O_5$ and $Ba_6Ti_{17}O_{40}$ in inter-granular regions but their volume fractions were too small to be detected *via* XRD. For powders produced at 180 °C, where the products appeared phase-pure by Raman spectroscopy, sintered pellets contained only a very small

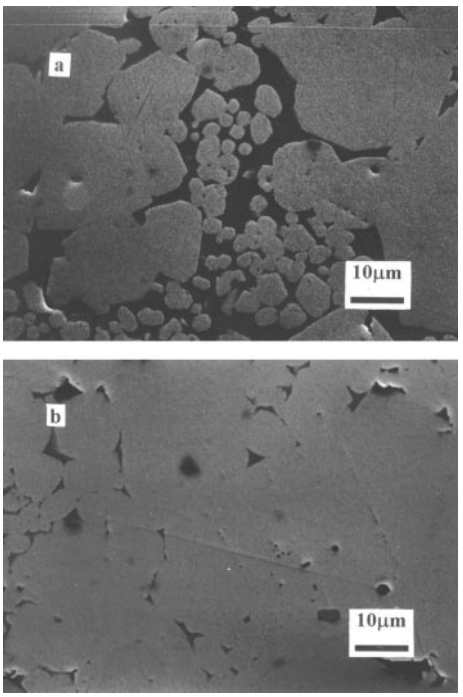

Fig. 9 Back scattered electron images of ceramic pellets sintered at 1350 °C from powders produced at 85 (a) and 180 °C (b).

volume fraction of $Ba_6Ti_{17}O_{40}$, as shown by the dark, isolated regions in the BSE image, Fig. 9(b).

The Ti-rich secondary phases in powders prepared at 85 °C are clearly associated with unreacted Ti-precursor, which reacts with surrounding $BaTiO_3$ particles at elevated temperatures to form Ti-rich binary phases. It is unclear, however, whether the secondary phase produced from powders prepared at 180 °C is associated with unreacted Ti-precursor which has not been detected *via* Raman spectroscopy (or analytical TEM) or is associated with a compositional Ba/Ti gradient within individual particles of the as-prepared powders.

Direct evidence of V_{Ba}'' on the surfaces of individual particles, either from incorporation of lattice hydroxyl ions during hydrothermal synthesis or *via* acid/aqueous media wet milling of powders has been limited. Abicht *et al.*[49] used HREM and EELS to demonstrate that the outer surfaces of individual $BaTiO_3$ particles which have been wet milled in aqueous media show evidence of Ba^{2+} leaching. They propose that a Ba/Ti concentration gradient exists within individual particles which consists of a 3–5 nm thick TiO_x-rich outer layer followed by a intermediate layer, *ca.* 10 nm thick, with a molar Ba/Ti ratio increasing from 0 to 1. These core-shell structures affect the sintering of $BaTiO_3$ powders due to the reactivity of the Ti-rich, outer layers. Our observation of small quantities of Ti-rich intergranular regions in sintered pellets of hydrothermal powders produced at 180 °C is consistent with this model but in-depth studies using HREM and EELS are required to establish the presence or absence of any Ba/Ti compositional gradient within individual particles of $BaTiO_3$ (produced *via* hydrothermal synthesis).

Heat treatment of hydrothermal powders at 1000 °C is sufficient to remove any adsorbed or structural water and create oxygen vacancies within the lattice, eqn. (3). It is insufficient, however, to cause substantial migration of barium vacancies or densification and grain growth *via* liquid phase sintering involving Ti-rich outer particle surfaces and/or any excess unreacted Ti-precursor material. Consequently, ceramic pellets formed at 1000 °C are poorly sintered, have low density, *ca.* 65% of the theoretical density, and consist of small grains with very poor inter-granular contact. Despite this the pellets exhibit exceptionally low room temperature resistivities, *ca.* 10–50 MΩ.

Complex impedance plane, Z^*, plots at 32 and 44 °C for a pellet sintered at 1000 °C are shown in Fig. 10. The plots consist of a high frequency semicircular arc with an associated capacitance of 32 pF and a low frequency-spike with an associated capacitance in the order of 1 μF. The capacitance value for the bulk or intra-granular component is consistent with a poorly sintered $BaTiO_3$ ceramic and the low frequency, inclined spike is attributable to ionic polarisation and diffusion-limited phenomena at the electrodes and supports the idea that conduction is mainly by means of ions at these temperatures.

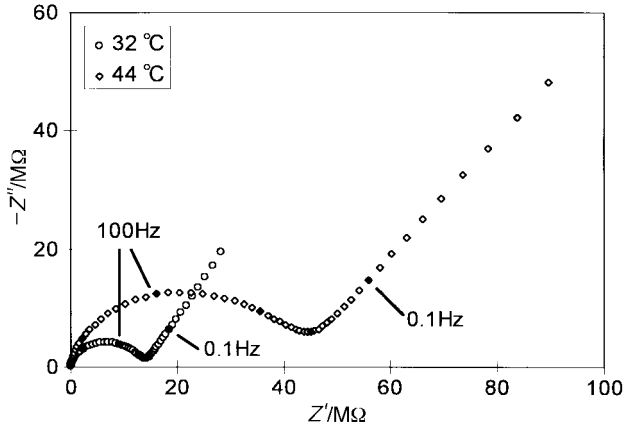

Fig. 10 Complex impedance plane plots at 32 and 44 °C for a pellet of powder prepared at 85 °C and sintered at 1000 °C. Selected frequencies (in Hz) are shown for filled symbols.

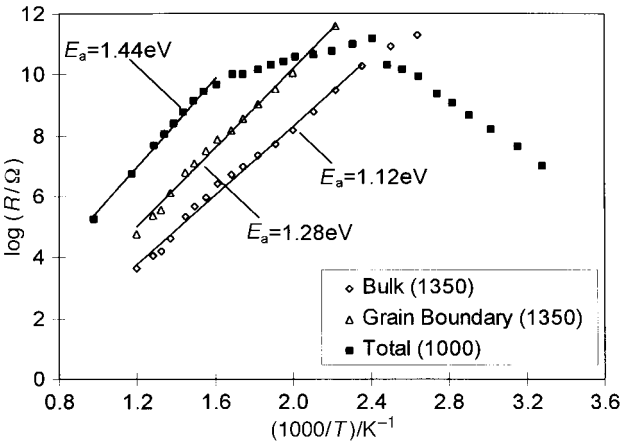

Fig. 11 Log resistivity *versus* 1000 K/T for pellets of powder prepared at 85 °C and sintered at 1000 °C (filled squares) and 1350 °C (open symbols). Calculated activation energies are in eV.

Bulk resistivity values were extracted from the low frequency intercept of the semi-circular arc with the Z' axis on the Z^* plots. Initially, the bulk resistivity increases on heating, as shown by the increase in diameter of the bulk semi-circular arc in the Z^* plots, Fig. 10, and in the log resistance, Arrhenius-type plot shown in Fig. 11. The bulk resistivity rises by several orders of magnitude on heating to *ca.* 150 °C, then remains temperature independent before decreasing in accordance with the Arrhenius law at temperatures above *ca.* 350 °C. In this high temperature region, there was no evidence of the low frequency, inclined spike in Z^*; instead, the plots consisted of a single, bulk semi-circular arc, indicating that conduction was predominantly electronic. The resistivity behaviour was reversible on thermal cycling. For comparison, bulk and grain boundary resistivities extracted from high and low frequency semicircular arcs in Z^* plots for a pellet sintered at 1350 °C are also shown in Fig. 11. These values are consistent with those reported in the literature for dense $BaTiO_3$ ceramics.[50] It should be noted that the room temperature resistivity of these ceramics is in excess of 1 TΩ and that no low frequency, inclined spike was observed in any Z^* plots.

The exceptionally low bulk resistivity value of 20 MΩ at 25 °C, the presence of a low frequency spike in Z^* plots below *ca.* 150 °C and the fact that resistivity initially rises with temperature, all indicate that $BaTiO_3$ prepared *via* hydrothermal synthesis at 85 °C and sintered at 1000 °C is a modest proton conductor, especially at temperatures close to room temperature. Presumably water vapour is adsorbed from the ambient on cooling (from the sintering temperature of 1000 °C) and partially reverses the reaction given in eqn. (3), thus, converting doubly ionised oxygen vacancies into lattice hydroxyl ions. Subsequent reheating removes water rather easily and the bulk resistivity increases rapidly; however, temperatures in excess of 350 °C are required before the predominant charge carriers are electronic. More detailed studies of this unusual bulk resistivity behaviour will be reported elsewhere,[51] however, such materials are clearly poor dielectrics.

To our knowledge, this is the first time that proton conduction has been demonstrated in oxygen-deficient $BaTiO_3$ materials. Many other oxygen-deficient perovskites such as doped, alkaline earth zirconates[52] and cerates[53] are well-known proton conductors. Several different mechanisms of incorporation of protonic defects in such oxides have been suggested,[54] involving interstitial protons and lattice hydroxyl ions,

$$H_2O\ (g) + V_O^{\bullet\bullet} \rightleftharpoons 2H_i^{\bullet} + O_O^x \quad (4)$$

$$H_2O\ (g) + O_O^x + V_O^{\bullet\bullet} \rightleftharpoons 2OH_O^{\bullet} \quad (5)$$

however, the detailed mechanism remains unclear.

Conclusions

Amorphous H_2TiO_3 is an excellent Ti-precursor to use in the hydrothermal synthesis of $BaTiO_3$. Phase pure powders with small particle sizes, *ca*. 40–80 nm and narrow particle size distributions can be prepared at 180 °C after 24 h. Although initial reaction is very fast, *ca*. 90% yield after 8–10 h, extended heating at 180 °C is required to drive reactions to completion. Lowering the reaction temperature produces powders with even smaller particle sizes but very long reaction periods are required, >72 h, to ensure complete reaction. In addition, the powders are poorly crystalline and have high water content.

In order to obtain phase pure $BaTiO_3$ ceramics it is important to control the Ba/Ti ratio. As the rate limiting step in the synthesis involves reaction of the Ti-precursor, it is important to use a technique which can detect very small quantities of unreacted amorphous or crystalline Ti-precursor material. We have clearly demonstrated that Raman spectroscopy, rather than XRD, is a simple and effective technique for this purpose.

Raman spectra of powders with an average particle size as small as *ca*. 20–40 nm indicate asymmetry within the TiO_6 octahedra of the $BaTiO_3$ lattice. This contradicts the widely cited 'critical' particle size theory for the stabilisation of the cubic polymorph, at least for particle sizes in excess of *ca*. 20–40 nm. Raman spectra of powders heat treated at *ca*. 1000 °C to remove adsorbed and structural water are very similar to that of as-prepared powders. This contradicts the suggestion that lattice hydroxyl ions stabilise the cubic polymorph of $BaTiO_3$ prepared *via* a wet chemical technique, such as hydrothermal synthesis. Finally, as-prepared powders contain many defects, primarily lattice OH^- ions. Preliminary conductivity results on pellets of powders which have been heated treated to remove lattice hydroxyl ions reveal these materials to be modest proton conductors at room temperature.

Acknowledgements

The authors would like to thank Dr Eric Lachowski for assistance with electron microscopy, Dr Alison Coats for EPMA, Dr Susan Blake for XRD, Mr James Marr for BET analysis and Professor Tony West for useful discussions. The EPSRC and AIST (Japan) are gratefully acknowledged for financial support.

References

1 B. Jaffe, W. R. Cook and H. Jaffe, *Piezoelectric Ceramics*, Academic Press, London, 1971.
2 D. Hennings, *Int. J. High Technology Ceramics*, 1987, **3**, 91.
3 G. Arlt, D. Hennings and G. de With, *J. Appl. Phys*., 1985, **58**, 1619.
4 M. H. Frey, Z. Xu, P. Han and D. A. Payne, *Ferroelectrics*, 1998, **206**, 337.
5 W. R. Bussen, L. E. Cross and A. K. Goswami, *J. Am. Ceram. Soc*., 1966, **49**, 33.
6 G. Arlt, *Ferroelectrics*, 1990, **104**, 217.
7 A. Morell and J. C. Niepce, *J. Mater. Educ*., 1991, **13**, 173.
8 T. Takeuchi, K. Ado, T. Asai, H. Kageyama, Y. Saito, C. Masquelier and O. Nakamura, *J. Am. Ceram. Soc*., 1994, **77**, 1665.
9 W. Kanzig, *Phys. Rev*., 1955, **98**, 549.
10 K. Kinoshita and A. Yamaji, *J. Appl. Phys*., 1976, **47**, 371.
11 M. Kataoka, K. Suda, N. Ishizawa, F. Marumo, Y. Shimizugawa and K. Ohsumi, *J. Ceram. Soc. Jpn*., 1994, **102**, 213.
12 K. Uchino, E. Sadanaga and T. Hirose, *J. Am. Ceram. Soc*., 1989, **72**, 1555.
13 F. J. Gotor, C. Real, M. J. Dianez and J. M. Criado, *J. Solid State Chem*., 1996, **123**, 301.
14 S. Schlag and H. F. Eicke, *Solid State Commun*., 1994, **91**, 883.
15 B. D. Begg, E. R. Vance and J. Nowotny, *J. Am. Ceram. Soc*., 1994, **77**, 3186.
16 H. I. Hsiang and F. S Yen, *J. Am. Ceram. Soc*., 1996, **79**, 1053.
17 R. Vivekanandan and T. R. N. Kutty, *Powder Technol*., 1989, **57**, 181.
18 K. Uchino, N. Lee, T. Toba, N. Usuki, H. Aburatani and Y. Ito, *J. Ceram. Soc. Jpn*., 1992, **100**, 1091.
19 F. Yen, C. T. Chang and Y. Chang, *J. Am. Ceram. Soc*., 1970, **73**, 3422.
20 J. Nowotny and M. Rekas, *Solid State Ionics*, 1991, **49**, 135.
21 D. Hennings, M. Klee and R. Waser, *Adv. Mater*., 1991, **3**, 334.
22 M. Mori and T. Kineri, *J. Am. Ceram. Soc*., 1995, **78**, 2391.
23 A. I. Kingon, S. K. Streiffer, C. Basceri and S. R. Summerfelt, *MRS Bull*., 1996, **6**, 46.
24 K. Wa. Gachigi, U. Kumar and J. P. Dougherty, *Ferroelectrics*, 1993, **143**, 229.
25 F. Chaput and J. P. Boilt, *J. Am. Ceram. Soc*., 1990, **73**, 942.
26 M. Demartin, C. Herard, C. Carry and J. Lemaitre, *J. Am. Ceram. Soc*., 1997, **80**, 1079.
27 W. Zhu, C. C. Wang, S. A. Akbar and R. Asiaie, *J. Mater. Sci*., 1997, **32**, 4303.
28 W. Zhu, C. C. Wang, S. A. Akbar, R. Asiaie, P. K. Dutta and M. A. Alim, *Jpn. J. Appl. Phys*., 1996, **35**, 6145.
29 A. Beauger, J. C. Mutin and J. C. Niepce, *J. Mater. Sci*., 1983, **18**, 3041.
30 A. Beauger, J. C. Mutin and J. C. Niepce, *J. Mater. Sci*., 1983, **18**, 3543.
31 J. C. Mutin and J. C. Niepce, *J. Mater. Sci. Lett*., 1984, **3**, 591.
32 A. Beauger, J. C. Mutin and J. C. Niepce, *J. Mater. Sci*., 1984, **19**, 195.
33 R. Asiaie, W. Zhu, S. A. Akbar and P. K. Dutta, *Chem. Mater*., 1996, **8**, 226.
34 W. S. Clabaugh, E. M. Swiggard and R. Gilchrist, *J. Res. Natl. Bur. Stand*., 1956, **56**, 289.
35 M. P. Pechini, *US Pat*., 3 330 697, 1967.
36 N. J. Ali and S. J. Milne, *Trans. J. Br. Ceram. Soc*., 1987, **86**, 113.
37 M. H. Frey and D. A. Payne, *Chem. Mater*., 1995, **7**, 123.
38 A. D. Hilton and R. Frost, *Key Eng. Mat*., 1992, **66/67**, 145.
39 M. M. Lencka and R. E. Riman, *Chem. Mater*., 1993, **5**, 61.
40 W. Hertl, *J. Am. Ceram. Soc*., 1988, **71**, 879.
41 J. O. Eckert Jr., C. C. Hung-Houston, B. L. Gersten, M. M. Lencka and R. E. Riman, *J. Am. Ceram. Soc*., 1996, **79**, 2929.
42 C. H. Perry and D. B. Hall, *Phys. Rev. Lett*., 1965, **15**, 700.
43 G. Busca, V. Buscaglia, M. Leoni and P. Nanni, *Chem. Mater*., 1994, **6**, 955.
44 D. Hennings and S. Schreinemacher, *J. Eur. Ceram. Soc*., 1992, **9**, 4.
45 S. Wada, T. Suzuki and T. Noma, *J. Ceram. Soc. Jpn*., 1996, **104**, 383.
46 R. Waser, *J. Am. Ceram. Soc*., 1988, **71**, 58.
47 I. J. Clark, T. Takeuchi, N. Ohtori and D. C. Sinclair, unpublished work.
48 M. H. Frey and D. A. Payne, *Phys. Rev. B*, 1996, **54**, 3158.
49 H. P. Abicht, D. Voltzke, A. Roder, R. Schneider and J. Woltersdorf, *J. Mater. Chem*., 1997, **7**, 487.
50 N. Hirose and A. R. West, *J. Am. Ceram. Soc*., 1996, **79**, 1633.
51 I. J. Clark and D. C. Sinclair, unpublished work.
52 H. Iwahara, T. Esaka, H. Uchida and N. Maeda, *Solid State Ionics*, 1981, **3/4**, 359.
53 H. Uchida, H. Yoshikawa and H. Iwahara, *Solid State Ionics*, 1989, **34**, 103.
54 K. D. Kruer, *Chem. Mater*., 1996, **8**, 610.

Paper 8/05756G